

Effects of the Geometry of Friction Interfaces on the Nonlinear Dynamics of Jointed Structure

Jie Yuan, Loic Salles, and Christoph Schwingshackl

Abstract Friction interfaces are commonly used in large-scale engineering systems for mechanical joints. They are known to significantly shift the resonance frequencies of the assembled structures due to softening effects and to reduce the vibration amplitude due to frictional energy dissipation between substructural components. It is also widely recognized that the geometrical characteristics of interface geometry have a significant impact on the nonlinear dynamical response of assembled systems. However, the full FE modeling approaches including these geometrical characteristics are extremely expensive. In this work, the influence of geometry of friction interfaces is investigated by using a multi-scale approach. It consists in integrating a semi-analytical contact solver into a high-fidelity nonlinear vibration solver. A highly efficient semi-analytical solver based on the boundary element method is used to obtain the pressure and gap distribution from the contact interface with different geometrical characteristics. The static pressure and gap distribution are then used as input for a nonlinear vibration solver to evaluate nonlinear vibrations of the whole assembled structure. The effectiveness of the methodology is shown on a realistic “Dogbone” test rig, which was designed to assess the effects of blade root geometries in a fan blade disk system. The friction joints with different interface profiles are then investigated. The obtained results show that the effects of the surface geometrical characteristics can have a significant impact on the damping and resonant frequency behavior of the whole assembly.

Keywords Friction interface · Nonlinear vibration · Multi-scale analysis · Contact mechanics · Nonlinear modal analysis

1 Introduction

Friction interfaces are widely used in large-scale engineering system that need to connect different sub-components. It is well-known that these interfaces have a significant impact on the dynamics of the assembled structure by shifting the resonance frequencies and effectively decreasing the vibration amplitude via strong energy dissipation. Because of the large damping effects, friction interfaces have been also widely exploited for the design of mechanical dampers, particularly in turbomachinery, where other types of dampers are generally infeasible due to the high temperature. Underplatform dampers (UPDs) [1] are one of these typical examples which are usually placed in the groove under the platforms of two adjacent blades. The energy dissipation from friction interfaces can effectively reduce the vibration level and mitigate the risk of high-cycle fatigue failures. Similar examples can also be found in the design of ring dampers for blisks [2]. However, an accurate prediction of the dynamics of the structure with friction interfaces remains a challenge due to complex physics at the friction interface [3].

Significant research efforts have been made in the last decade to better understand the role of friction interfaces in the nonlinear dynamical response, particularly for UPDs. Petrov [4] and Krack [5] carried out a sensitivity analysis of UPD designs to contact parameters at the blade-damper interface including the normal loads. Tang and Epureanu [6] investigated the effects of geometric parameters of a V-shaped friction ring damper on the turbine blade. Panning et al. studied the influence of the contact geometry on the damping effectiveness by parametrically varying both the geometry of the blade platform and the damper [7]. Hüls investigated the effects of geometric parameters of turbine friction dampers on the nonlinear vibration response [8]. To consider the fretting wear effects, Gallego carried out multi-scale computation of fretting

J. Yuan (✉) · L. Salles · C. Schwingshackl

Vibration University Technology Centre, Department of Mechanical Engineering, Imperial College London, London, UK
e-mail: jie.yuan@imperial.ac.uk; l.salles@imperial.ac.uk; Christoph.Schwingshackl@imperial.ac.uk

wear at the interfaces in a bladed disk system [9]. Armand implemented a multi-scale approach to quantify the effects of the surface roughness and fretting wear at the friction interface on the nonlinear dynamic response [3]. Delaune et al. also investigated the impact of fretting wear and showed that a large variety of vibration behaviors can be observed when wear effects are considered [10]. Recently, Gastaldi et al. experimentally investigated the effect of surface finish on the functioning of UPD showing a large impact of the contact interface conditions on the dynamic response [11]. All these studies have indicated that the topology of friction interfaces has a big influence on the dynamics of structures with friction interfaces. However, most of the previous studies have focused on the effects of the contact parameters or macro-scale geometries. The effects of surface geometry at the contact interface have not been thoroughly investigated due to high computational expense, because an extremely dense mesh would be required to model these interface profiles making the nonlinear dynamic analysis infeasible.

To address this problem, this paper employs a multi-scale modeling approach to study the effects of the interface geometry and improve the dynamic design of jointed structures. The main idea of this approach is that, instead of directly using a dense mesh in FEA, a semi-analytical solver is used for the highly refined nonlinear contact analysis of the interface with different profiles. In this way, one can significantly reduce the high computational cost by avoiding using dense meshes for the FE analysis. The paper will firstly present the methodology of this multi-scale approach; it is followed by the presentation of a realistic test case, where four different interface profiles will be evaluated and compared.

2 Methodology

The general structure of the multi-scale modeling approach is described in Fig. 1. This approach includes nonlinear dynamic/static analysis based on a macro-scale model and nonlinear contact analysis based on a “micro-scale” interface. The “micro-scale” refers to the interface with extremely fine mesh that is sufficient to represent the interface profiles. The nonlinear static analysis (with a flat-on-flat contact interface) is firstly performed to evaluate overall contact loads on the friction interfaces. With these contact loads, refined contact analysis is then carried out based on a semi-analytical solver, which can effectively consider the variation of interface profiles. The normal and gap distribution on the friction interfaces is then obtained at a very low computational cost. The distributions of these contact loads are then interpreted and then upscaled as the input for further nonlinear dynamic analysis of the macro-scale FE model. In this way, the effects of different interface profiles on the nonlinear dynamics can be evaluated efficiently without the need to re-mesh the contact surface for each profile. The nonlinear dynamic analysis can be still performed on the same macro-scale model to save the computational cost. This approach is mainly based on an assumption that the variation of micro-scale surface geometries does not change the overall contact loads at the contact interfaces.

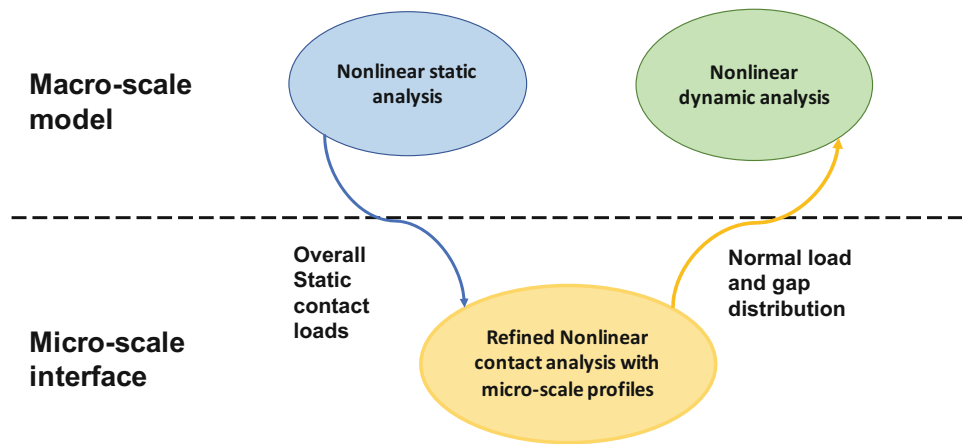


Fig. 1 A general structure of the multi-scale approach

2.1 Step 1: Nonlinear Static Analysis

A nonlinear static analysis is initially performed on a macro-scale FE model to identify the nonlinear static equilibrium condition. The purpose of this analysis is to obtain the overall contact loads at the contact interfaces. As shown in Eq. (1), \mathbf{K} represents the linear stiffness of the joint stiffness; f_{nl} is the nonlinear contact force from the mechanical joints, which is dependent on the displacement and velocity of the interface DOFs; $F_s(t)$ is the static loading applied to the system. This nonlinear contact analysis can be carried out using any commercial software, e.g., Abaqus, where the surface-on-surface hard contact is fined on the interface. As a result, the distribution of normal contact loads on the contact load can be extracted:

$$\mathbf{K}X(t) + f_{nl}(X(t), \dot{X}(t)) = F_s(t) \quad (1)$$

The identified loads from the interface will then be used for a refined contact analysis, including different micro-scale interface profiles.

2.2 Step 2: Refined Contact Analysis

A refined contact analysis with a dense mesh is then performed by the means of an already available semi-analytical boundary element solver [3]. The contact solver is essentially based on the projected conjugate gradient method and a discrete-convolution fast Fourier transform which speeds up the computation. The half-space assumption allows the use of the Boussinesq and Cerruti potentials to compute the surface elastic deflections in the normal and tangential direction. Thanks to the computational speed of this contact solver, a very refined contact mesh can be used, which allows to include roughness and surface profiles into the analysis. The normal displacement u_z caused by a pressure distribution p is described in Eq. (2), whereas Eq. (3) is its discretized form on a regular grid of $N_x \times N_y$ points:

$$u_z(x, y) = \frac{1 - \nu^2}{\pi E} \int_{-\infty}^{+\infty} \int_{-\infty}^{+\infty} \frac{p(\xi, \eta)}{\sqrt{(\xi - x)^2 + (\eta - y)^2}} d\xi d\eta \quad (2)$$

$$u_z(i, j) = K_{zz} \otimes p = \sum_{k=1}^{N_x} \sum_{l=1}^{N_y} p(k, l) K_{zz}(i - k, j - l) \quad (3)$$

where E and ν are Young's modulus and Poisson ratio of the material, respectively, \otimes is the discrete convolution product, and $K_{zz}(i, j)$ are the discrete influence coefficients which are used to obtain the normal displacement resulting from unit pressure on the element (i, j) . Initially, the normal contact problem is solved using the conjugate gradient method, after which the tangential problem is solved with the Coulomb friction law as a bound to the shear distribution in the slipping region.

As a result, the distribution of normal contact loads and gap between contact surfaces can be effectively obtained for the contact surface including the effects of micro-scale interface profiles. These distributions are then interpolated for the macro-scale FE model for nonlinear dynamic analysis with respect to Newton's third law making sure the force and moment are equivalent on the whole interface.

2.3 Step 3: Nonlinear Dynamic Analysis

Nonlinear dynamic analysis is then carried out for the macro-scale FE model with the input contact loads from interpolated micro-scale profiles. The equation of motion for the dynamic analysis is shown in Eq. (4):

$$\mathbf{M}\ddot{X}(t) + \mathbf{K}X(t) + f_{nl}(X(t), \dot{X}(t)) = F_d(t) \quad (4)$$

where $F_d(t)$ is the dynamical loading in the system and \mathbf{M} is the linear mass matrix of the jointed structure. 3D node-to-node contact element is used to model the contact friction between the surfaces, which combines two Jenkins elements (in contact plane), and a unilateral spring is used to describe the normal contact forces between the contacting surfaces [12]. Instead of using forced frequency analysis, damped nonlinear modal analysis (dNNM) is employed. The advantage of using dNNM analysis is that it can directly and efficiently calculate resonance frequency and damping with a wide range of energy levels. In this study, the extended periodic motion concept, proposed by Krack [13], is used for dNNM analysis. In contrast to complex nonlinear modal analysis [14], the used approach is also suitable when the system has a large damping value. As shown in Eq. (5),

$$a (\mathbf{M}\ddot{\mathbf{X}}(t) - 2\zeta\omega_0\mathbf{M}\dot{\mathbf{X}}(t) + \mathbf{K}\mathbf{X}(t)) + f_{nl}(\mathbf{X}(t), \dot{\mathbf{X}}(t), a) = 0 \quad (5)$$

An artificial damping ζ is introduced to make the nonconservative system periodic by balancing the energy dissipated from the nonlinear contact force; a is the modal amplitude indicating the level of input energy in the system. A well-established HBM framework [15] is then used to compute the steady-state dynamics for different modal amplitudes. The modal amplitude can then be interpolated as an equivalent force level F_d by using the extended-energy balance method [17].

3 Case Study

The presented FE joint model for the case study is based on an available blade root test rig setup [16]. In this assembly, a particular blade root design is machined onto both ends of a beam (“Dogbone”), which is then fitted between two clamps, and put into tension to simulate the in-rotation centrifugal loading that occurs due to rotation. The Dogbone test rig shown in Fig. 2(a) consists of two main components: a set of identical solid root-block disks and a set of “bones” for different root designs. The disks shown in Fig. 2(b) are 16-sided with currently five adjacent sides used to house different blade root designs. A rounded and hardened central bore in the disk provides a near-point contact with a hardened U-shaped hook which holds the clamping disk in place. This arrangement was chosen in an attempt to minimize the damping introduced by the supporting structure. In this case study, a root design similar to a dovetail joint in a fan blade disk is considered, which is shown in Fig. 2(c). In terms of FE modeling, the disks on both sides are simplified as one cyclic sector to reduce the computational expense. There are four contact interfaces where two are on the top disk and the other two on the bottom disk. The size of friction interface is 18 mm × 1.6 mm. For each friction interface, there are 28 nonlinear elements involving 40 contact nodes. Figure 2(d) shows the first bending mode of the test rig from a linear dynamic analysis, which will be the focus of this study.

Figure 3(a) shows the root geometry of the bone in Fig. 2, where the contact surface is in blue. Figure 3(b–d) shows three different “micro-scale” interface geometries which will be investigated in this study. They will be referred to as Y-wise bump,

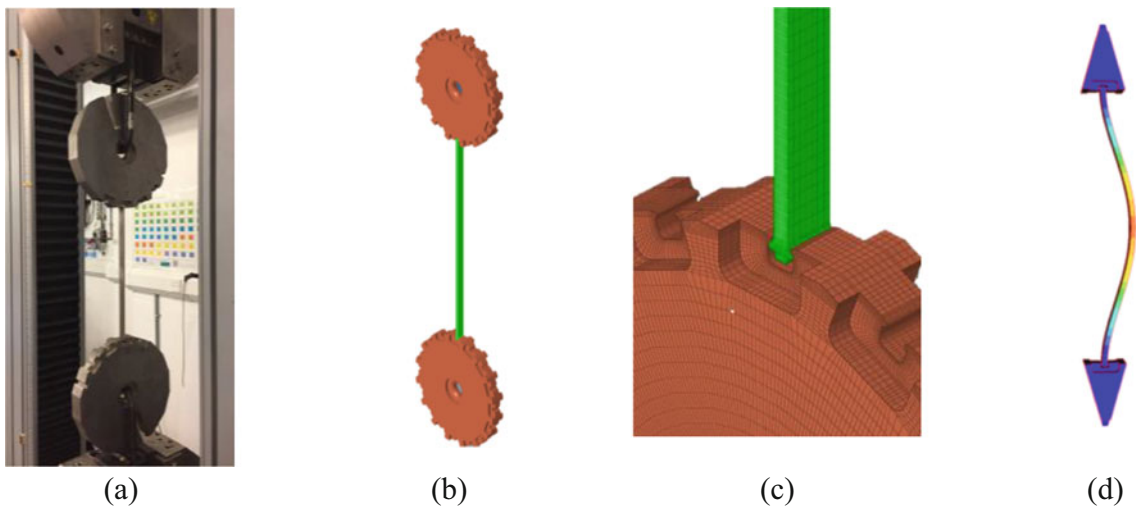


Fig. 2 (a) Experiment setup, (b) 3D full-scale FE model, (c) zoomed dovetail joint, (d) first bending mode

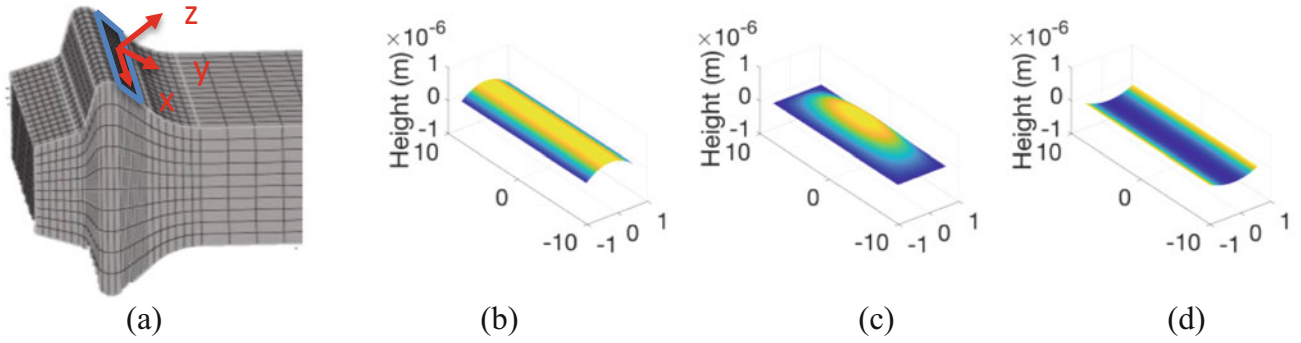


Fig. 3 (a) Root geometry; (b) Y-wise bump; (c) Center bump; (d) Y-wise concave

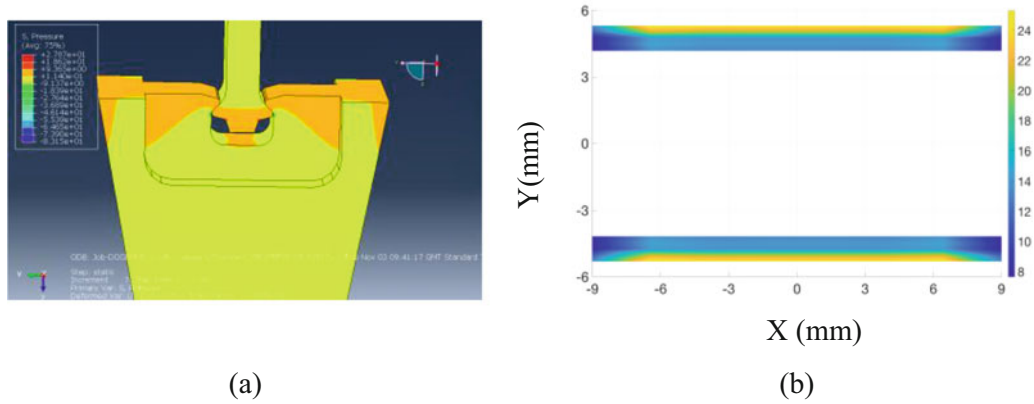


Fig. 4 Nonlinear static analysis: (a) pressure distribution in joints, (b) pressure distribution on the contact surface (Pa)

center bump, and Y-wise concave respectively. The maximum height of these interface geometries is around $1 \mu\text{m}$. These profiles are introduced to the blade (bone) interface, while the friction interfaces on the disks remain flat. The flat-to-flat contact interface is also investigated for reference. All four friction interfaces on the bone have the same profile.

4 Results

Figure 4(a) shows the results from a nonlinear static analysis of the Dogbone test rig with a flat-to-flat interface. The simulation was performed in Abaqus using surface-to-surface hard contact. In terms of pre-loading, the end of one disk is fully fixed, and a pulling loading of 1000 N is applied at the end of the other disk, which is equivalent to the loading applied during the experiment. Figure 4(b) shows the distribution of the extracted normal pressure loads at two friction interfaces from the disk on the bottom. It is clear that the normal contact pressure is localized on the downward sides of the interfaces, which is because the blade root is opening up a bit when the Dogbone is pulled up. It is also found that there is no gap appearing on these two friction interfaces. The pressure distribution is the same for all four friction interfaces (top and bottom) due to the symmetry of the test rig and loading conditions. All the pressure distributions are summed up to form an equivalent force vector applied at the center of the interface for the analysis in SAM, including forces in three directions and bending moment in three directions.

Figure 5 shows the pressure distribution from the refined contact analysis with the semi-analytic solver for different interface profiles described before. Herein, it is assumed that the overall contact load would remain unchanged for different micro-scale contact interfaces. They are all computed at a refined grid of 250×125 points for each friction interface instead of 8×5 points used in FE model. The computation for each profile only takes around 20s. As expected, for the Y-wise bump profile, the pressure is localized in the middle of interface; the pressure is centralized for the central bump profile, while the Y-wise concave profile leads to edgewise localized pressures. The pressure distributions are then interpolated to the much rougher nonlinear dynamic mesh to form the inputs for nonlinear dynamic analysis.

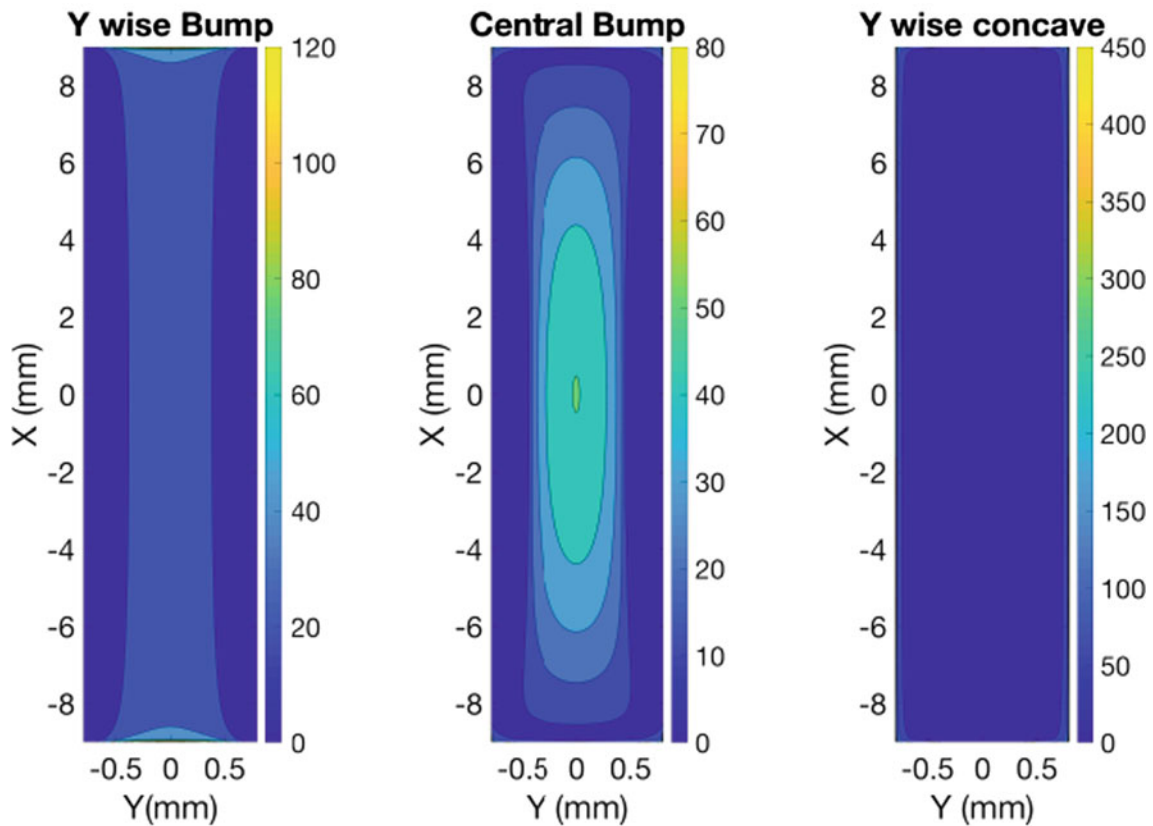


Fig. 5 Pressure distribution at the friction interface

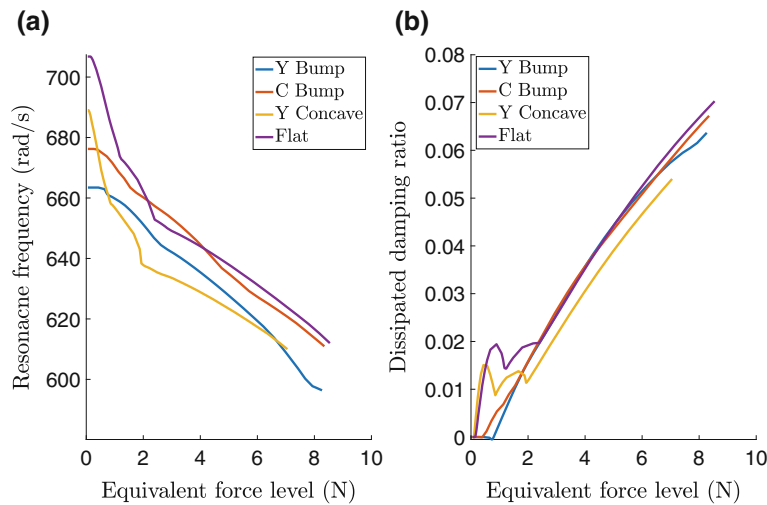


Fig. 6 The results from damped nonlinear modal analysis. (a) Resonance frequency and (b) dissipated damping ratio

Figure 6 shows the results from the dNNM analysis using harmonic balance method. Instead of showing the modal amplitudes, the equivalent force level is calculated by the extended-energy balance method assuming the forcing position is applied in the middle of the bone and at the out-of-plane direction. As expected, the global trend is similar for these four interface profiles. The resonance frequencies decrease in all four cases with the forcing level due to increasing softening effects at the friction interface, and the damping ratio increases with the excitation levels for all four profiles. However, the gradient of these two quantities to force levels during the stick-slip transition is very different for these four interface profiles. For the flat and Y concave profile, both the resonance frequency and damping ratio change rapidly once the slipping

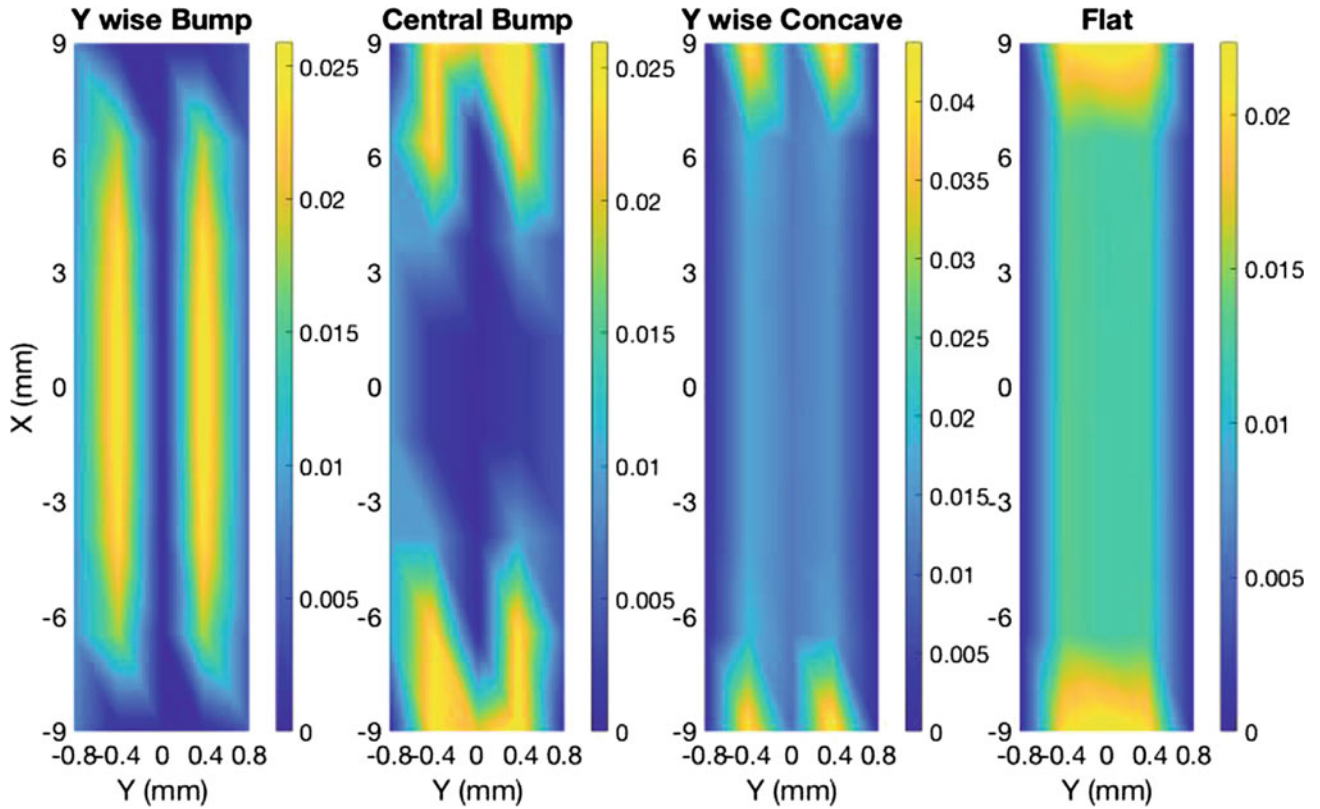


Fig. 7 Energy dissipation on the friction interface at the equivalent force level of 2 N

condition is triggered. It is mainly because the normal pressure of these two geometries is both localized on the edges of the interface. In comparison, they change much gradually for the Y and C bump as the contact pressure spreads over a wider contact zone leading to a lower pressure peak. One can also see that the starting resonance frequency for Y and C bump is much lower than Y concave and flat interface. This is because the bump profiles would leave a lot of gaps or much lower pressure on the edges, which will reduce the joint stiffness. One can also observe some difference in damping in Fig. 6b. The bump interfaces have a steady damping increase with excitation levels, while the other two have a steep and unsteady increase at low excitation levels. Figure 7 shows energy dissipation on the contact interface for these four interface profiles at an excitation level of 2 N. As expected, the distribution of dissipated energy varies quite a lot for different surface geometries and is consistent with pressure distribution shown in Fig. 5. Overall, the frequency drop due to the interface geometry can be up to 5.7% and the damping increase can be up to 0.02 with different interface profiles. It means that the variation of these nonlinear dynamic parameters is highly sensitive to the micro-scale interface topology through its significant impact on the distribution of normal pressure and gap at the contact interfaces.

5 Conclusion

The objective of the work was to present a multi-scale-based methodology to efficiently evaluate the effects of micro-scale interface geometries on the nonlinear dynamical response of a structure with frictional interfaces. This approach is based on combining a macro-scale FE model for nonlinear dynamic analysis with a micro-scale friction interface model for the quasi-static nonlinear contact analysis. The main advantage of the approach is that, instead of directly using FE models to include often minute interface profiles, a highly efficient semi-analytical contact solver is used. It can efficiently evaluate the influence of interface profiles on the contact pressures at a much lower cost. The resulting contact pressure and gap distribution are then fed as inputs into the macro-scale FE model to evaluate the nonlinear dynamical response with an HBM solver. The proposed approach was applied to the design of a new blade root Dogbone test rig, to evaluate the effects of blade root geometries on the overall dynamic response of the system. Four different interface profiles were investigated. The

obtained results have shown that the effects of micro-scale interface profiles can have a significant impact on the damping and resonant frequency behavior, which should not be ignored in the dynamic prediction. The surface geometry may also be used as the design parameters to achieve robust and better dynamic performance of complex and nonlinear systems. The multi-scale approach has proven to be a very efficient method to simulate the effects of interface profiles on the nonlinear dynamical response.

Acknowledgments The authors would like to acknowledge the financial support from the EPSRC under SYSDYMATS project, Grand Ref: EP/R032793/1.

References

1. Yuan, Y., Jones, A., Setchfield, R., Schwingshackl, C.W.: Robust design optimisation of underplatform dampers for turbine applications using a surrogate model. *J. Sound Vib.* **494**, 115528 (2020)
2. Sun, Y., Yuan, J., Denimal, E. and Salles, L.: Nonlinear modal analysis of frictional ring damper for compressor Blisk. In: *Turbo Expo: Power for Land, Sea, and Air*. American Society of Mechanical Engineers (2020)
3. Armand, J., Salles, L., Schwingshackl, C.W., Süß, D., Willner, K.: On the effects of roughness on the nonlinear dynamics of a bolted joint: a multiscale analysis. *Eur J Mech A Solid*. **70**, 44–57 (2018)
4. Petrov, E.P.: Direct parametric analysis of resonance regimes for nonlinear vibrations of bladed disks. *J. Turbomach.* **129**(3), 495–502 (2006)
5. Krack, M., Tatzko, S., Panning-von Scheidt, L., Wallaschek, J.: Reliability optimization of friction-damped systems using nonlinear modes. *J. Sound Vib.* **333**(13), 2699–2712 (2014)
6. Tang, W., Epureanu, B.I.: Geometric optimization of dry friction ring dampers. *Int J Nonlinear Mech.* **109**, 40–49 (2019)
7. Panning, L., Sextro, W., Popp, K.: Optimization of the contact geometry between turbine blades and underplatform dampers with respect to friction damping. In: *Proceedings of the ASME Turbo Expo 2002: Power for Land, Sea, and Air*. Volume 4: Turbo Expo 2002, Parts A and B. Amsterdam, The Netherlands, pp. 991–1002
8. Gallego, L., Fulleringer, B., Deyber, S., Nelias, D.: Multiscale computation of fretting wear at the blade/disk interface. *Tribol. Int.* **43**(4), 708–718 (2010)
9. Hüls, M., Panning-von Scheidt, L., Wallaschek, J.: Influence of geometric design parameters onto vibratory response and high-cycle fatigue safety for turbine blades with friction damper. *J. Eng. Gas Turbines Power.* **141**(4) (2019)
10. Delaune, X., de Langre, E., Phalippou, C.: A probabilistic approach to the dynamics of wear tests. *J. Trib.* **122**(4), 815–821 (2000)
11. Gastaldi, C., Berruti, T.M., Gola, M.M.: The effect of surface finish on the proper functioning of underplatform dampers. *J. Vib. Acoust.* **142**(5) (2020)
12. Salles, L.C., Blanc, L., Thouverez, F., Gousskov, A.M., Jean, P.: Dynamic analysis of a bladed disk with friction and fretting-wear in blade attachments. *ASME Turbo Expo 2009: Power for Land, Sea, and Air*, Jun 2009, Orlando, vol. 48876, pp. 465–476 (2009)
13. Krack, M.: Nonlinear modal analysis of nonconservative systems: extension of the periodic motion concept. *Comput. Struct.* **154**, 59–71 (2015)
14. Laxalde, D., Thouverez, F.: Complex non-linear modal analysis for mechanical systems: application to turbomachinery bladings with friction interfaces. *J. Sound Vib.* **322**(4–5), 1009–1025 (2009)
15. Krack, M., Salles, L., Thouverez, F.: Vibration prediction of bladed disks coupled by friction joints. *Arch Comput Methods Eng.* **24**(3), 589–636 (2017)
16. Schwingshackl, C.W., Zolfi, F., Ewins, D.J., Coro, A., Alonso, R.: Nonlinear friction damping measurements over a wide range of amplitudes. In: *Proceedings of the international modal analysis conference XXVII*, Orlando (2009)
17. Sun, Y., Vizzaccaro, A., Yuan, J., Salles, L.: An extended energy balance method for resonance prediction in forced response of systems with non-conservative nonlinearities using damped nonlinear normal mode. *Nonlinear Dynamics.* **103**, 3315–3333 (2020)